Journal of Thermal Analysis and Calorimetry (2024) 149:8631–8645
https://doi.org/10.1007/s10973-024-13329-8

Effects of hybrid ZnO-WO_3/water nanofluid on the performance of active solar still equipped with a heat exchanger

Bandar Awadh Almohammadi[1] · Mathkar A. Alharthi[2] · Rayed S. Alshareef[2] · M. A. Sharafeldin[3] · H. A. Refaey[1,3] · H. A. Abd El-Ghany[4,5]

Received: 23 February 2024 / Accepted: 18 May 2024 / Published online: 24 June 2024

Abstract

Water is the secret of life. People demand more and more water. Solar stills generate distilled water. The present project involved designing and evaluating a heat exchanger-connected solar collector and solar still system. The effects of nanofluids on solar collector performance and solar still productivity were studied. Hybrid and mono ZnO/WO_3- water nanofluids have been produced in two steps. Individual and mixed nanofluids have a volume concentration of 0.035%. Four hybrid nanofluids with varying ZnO and WO_3 concentrations were examined. Nanofluid stability has been established. The thermal conductivity of nanofluids increased by 5.18–24.8%. The thermal optical efficiency of the solar collector was 0.708, with energy removal parameters of 34.888. The heat removal factor was raised to 0.8 for mono ZnO nanofluid. At a concentration of 0.035%, ZnO/water nanofluid can produce 3.14 kg of distilled water daily. The solar still's total efficiency, including pump consumption, was 39.9% for mono ZnO and 36.4% for WO_3. The highest efficiency received for hybrid ZnO + WO_3 nanofluids were 37.6%, 37.9%, 38.6%, and 39.2% for ZnO 0.01% + WO_3 0.025%, 0.015% + WO_3 0.022%, 0.025% + WO_3 0.015%, and 0.025% + WO_3 0.01%, respectively. As the ZnO percentage rose in hybrid ZnO + WO_3 nanofluids, energy absorption, thermal conductivity, solar still productivity, and efficiency were promoted.

Keywords Hybrid nanofluid · Active solar still · ZnO-WO_3/water · Heat exchanger

List of symbols

A_c	Solar collector area (m^2)	G_T	Normal solar radiation (W m^{-2})
A_s	Area of evaporation for solar still (m^2)	h_{fg}	Water vapor latent heat (kJ kg^{-1})
C_p	Heat capacity (J kg^{-1} K^{-1})	k_{nf}	Nanofluid thermal conductivity (W m^{-1} K^{-1})
F_R	Heat removal factor	k_{bf}	Base fluid thermal conductivity (W m^{-1} K^{-1})

✉ M. A. Sharafeldin
mahmoud.hassan@feng.bu.edu.eg

✉ H. A. Refaey
hrefaey@taibahu.edu.sa; hassanein.refaey@feng.bu.edu.eg

Bandar Awadh Almohammadi
bmohamdi@taibahu.edu.sa

Mathkar A. Alharthi
maaharthi@taibahu.edu.sa

Rayed S. Alshareef
rshreef@taibahu.edu.sa

H. A. Abd El-Ghany
hytham.abdelghany@feng.bu.edu.eg

[1] Department of Mechanical Engineering, College of Engineering at Yanbu, Taibah University, 41911 Yanbu Al-Bahr, Saudi Arabia

[2] Department of Chemical Engineering, College of Engineering at Yanbu, Taibah University, 41911 Yanbu Al-Bahr, Saudi Arabia

[3] Department of Mechanical Engineering, Faculty of Engineering at Shoubra, Benha University, Cairo 11629, Egypt

[4] Department of Physics, College of Science, Taibah University, Yanbu, Saudi Arabia

[5] Department of Engineering Mathematics and Physics, Faculty of Engineering at Shoubra, Benha University, Cairo 11629, Egypt

k_{np}	Nanoparticles thermal conductivity (W m^{-1} K^{-1})
$\dot{m}$ Nanofluid mass fl	Ow rate (kg s^{-1})
$\dot{m}_{ew}$	Hourly productivity (kg m^{-2} h^{-1})
Q_u	Useful rate of heat energy (W)
T_a	Ambient temperature (K)
T_i	Collector inlet temperature (K)
T_o	Collector outlet temperature (K)
T_w	Water temperature (K)
T_g	Glass temperature (K)
U_LOverall coeffi	Cient of heat loss (W m^{-2} K^{-1})
$V^{\bullet}$	Volume flow rate (m^3 h^{-1})

Greek symbols

α	The absorbance of the solar collector
η_i	Instantaneous efficiency
$\eta_{overall}$	Overall thermal efficiency included pump power consumption
ρ	Density (kg m^{-3})
τ	The transmittance of the collector glass
φ	Nanoparticles volume fraction

Subscripts

bf	Base fluid
nf	Nanofluid
np	Nanoparticles

Introduction

Clean water is continuously required for human uses, including drinking, farming, and industry. However clean water supplies are scarce in many nations, particularly in Asia and Africa. Many strategic papers warned that if the water scarcity problem remains unsolved, water wars may break out. To solve that issue, numerous researchers have attempted to improve the performance of solar stills.

Investigating the performance of the solar still in conjunction with a solar collector is one of the key concepts used by researchers. To improve the system's efficiency and water output, solar collectors served as preheaters in many research papers such as. Rajaseenivasan et al. [1] compared solar stills with and without a flat plate collector. They found that the water flow increased by 60% when they used the flat plate collector. Feilizadeh et al.'s study [2] looked at how different collector-to-basin area ratios affected the performance of multi-stage solar stills. Sharshir et al. [3] used evacuated tubes, an external condenser, nanoparticles, and ultrasonic foggers to increase the efficiency of solar stills. They discovered that adding just 1 mass percent of carbon black nanoparticles might increase the thermal efficiency of the particles by 28.2%. When Sheeba et al. [4] linked solar to a flat plate collector, the daily efficiency increased by 20.4%. Manokar et al. [5] investigated the efficacy of an active inclined solar panel basin solar still. Al-Molhem and Eltawil [6] studied the solar still in conjunction with a solar collector employing floatable black wicks in the sun still. Abdullah et al. [7] tested a solar still equipped with sands kinds and found its effect on freshwater productivity. Shaikh, and Ismail [8] studied theoretically a humidification–dehumidification water desalination system integrated with a flat plate solar water collector. Bafakeeh et al. [9] examined several nano-powders of MWCNTs and Al_2O_3 inside PCMs to enhance the thermal energy output of solar water desalination applications.

Menon [10] studied how water depth, still direction, and sun radiation affected the efficiency of a solar still linked to a flat plate solar collector. The findings revealed a 12% boost in efficiency. Narayana and Raju [11] described the effects of connecting one, two, or three flat plate collectors to a solar still. They discovered that one, two, and three flat plate collectors produced 2.669, 3.581, and 4.229 kg of distilled water, respectively. Abdullah et al. [12] studied the use of graphene quantum dots nanofluid in the production of solar stills. Efficiency was 87%, according to the results. Maatki [13] discovered that the influence of nanofluid concentration on heat transfer enhancement is affected by the operating circumstances of the solar still. Soliman et al. [14] investigated the performance of a solar still with an integrated heat exchanger in conjunction with an evacuated tube solar collector and a flat plate, both experimentally and conceptually. The results showed that utilizing an evacuated tube solar collector as a preheater for solar still is preferable to using a flat plate. Baharin et al. [15] showed that using a flat plate collector as a preheater raises the productivity of solar still, and it may be doubled. Parsa et al. [16] did an experimental investigation to determine the ideal level of nanoparticles (silver, 1–5%) in solar absorbers in the warmer months of the year with or without mirrors. The performance of the systems was carefully analyzed to determine the optimum concentration from a variety of angles, including energetic, exergetic, financial, productivity, exergoeconomic, efficiency, and environmental considerations for each season and during its existence. Balamurugan et al. [17] used a solar still in conjunction with an evacuated tube solar collector to investigate water production at various brine depths. To increase the efficiency of solar desalination, Shoeibi et al. [18] employed porous media, nano-enhanced phase transition materials, and nano-enhanced absorption (nano-coated). Abu-Arabi et al. [19] discovered that solar still paired with a solar collector and phase change material lowered water production as the phase change material to water mass ratio increased from 10 to 100%. Rai and Tiwari [20] investigated the performance of a solar still using a flat plate collector

in the short term. They discovered a 24% improvement in production. Morad et al. [21] investigated active and passive solar stills on a double slope. The active sun still productivity was 10.06 L m^{-2} day^{-1}, and passive solar still production was 7.8 L m^{-2} day^{-1}, respectively. The efficiency of active and passive solar stills was 80.6% and 57.1%, respectively.

Nanofluids are novel fluids that contain nanoparticles added to base fluid. Nanoparticles are used in a variety of applications due to their exceptional thermal properties. One of these applications is solar water distillation, as are the others listed below. Jathar and Ganesan [22] investigated the performance of a stepped solar still using MgO, Al_2O_3, and TiO_2 nanoparticles. Their volume concentrations were 0.1 and 0.2%, respectively. The water productivity with MgO, Al_2O_3, and TiO_2 nanoparticles increased by 51.28, 39.24, and 25.37%, respectively. Sharshir et al. [23] created a pyramid solar still that is connected to evacuated tubes and added CuO nanoparticles. Freshwater output increased by 26.6%, according to the findings. Saleh et al. [24] conducted an experimental investigation to determine the influence of ZnO nanoparticles on solar still production.

According to Elango et al. [25], the solar still with Aluminum Oxide (Al_2O_3)-water nanofluid boosted productivity by 29.95% when compared to Zinc Oxide (ZnO)-water nanofluid. Kabeel et al. [26] showed that employing nanofluids increased solar still water production by around 116% in the case of a still fitted with an external condenser. El-Gazar et al. [27] investigated an alumina-copper oxide hybrid nanoparticle (Al_2O_3-CuO). Each nanoparticle had a nanofluid concentration of 0.025%. According to the findings, utilizing hybrid nanofluid boosts solar still daily production to 5.5239 kg m^{-2} day in summer and 3.1079 kg m^{-2} day^{-1} in winter. The still improved by 27.2% and was 21.7% better than the solar still without nanoparticles. Kandeal et al. [28] used CuO nanoparticles in solar still to boost the thermal conductivity of water and PCM while affecting their specific heat just a little. The usage of SiO_2/water nanofluids as the running fluid in the heat exchanger boosted the solar still performance by around 10%, according to Mahian et al. [29]. Subhedar et al. [30] examined the influence of water and Al_2O_3/Water nanofluid at volume concentrations of 0.05% and 0.1% as working fluids in a standard single slope solar still plant with a parabolic trough collector. According to El-Ghetany et al. [31], utilizing TiO_2 nanoparticles at a concentration of 100 mg/l increases daily distilled water production by 26.9%. Akilu et al. [32] showed that reinforcing a G/EG mixture with 80% SiO_2 and 20% CuO/C increased thermal conductivity and viscosity by 26.9% and 1.15 times, respectively. Sadeghi and Nazari [33] tested the performance of a modified single slope solar still coupled to an evacuated tube collector with varied concentrations of antibacterial-magnetic Ag@Fe_3O_4/deionized water hybrid nanofluid. Visconti et al. [34] created a programmable electronic system for monitoring environmental parameters and controlling the electrical functions of a thermo-solar plant. The created control unit observes data from temperature and light sensors, processes the information, and orders other devices (pumps, electric valves, and power supplies) to improve plant efficiency. Gianpiero et al. [35] investigated the thermal performance of an innovative nanofluid solar thermal collector using commercial software (RadTherm Thermo-Analytics rel. 10.5). Al_2O_3-nanofluid was simulated as the solar thermal collector's working fluid, with nanoparticle concentrations ranging from 0%vol (pure water) to 3%vol of Al_2O_3 nanoparticles. The chemical stability, dynamic viscosity, FT-IR spectra, cluster size, and thermal conductivity of Al_2O_3-Therminol nanofluid as a working fluid in high-temperature solar energy systems were tested by Colangelo et al. [36]. Narendran et al. [37] stated the application of novel nanoplatelet-based vanadium pentoxide (V_2O_5)-xerogel for conjugate cooling in densely packed electronic devices. In Rayleigh–Benard (R-B) convection with air, water, and alumina-water nanofluid as working fluids, laminar natural convection, and entropy generation were incorporated by Karki et al. [38].

Although researchers made a great effort, many novel ideas can be applied to overcome pure water shortage. Based on our review and Xiong et al. [39], Rashidi et al. [40], Yang et al. [41], Al-Kayiem et al. [42], Jathar et al. [43], Tuly et al. [44], Bait et al. [45], Iqbal et al. [46], Naveenkumar et al. [47], and Akkala et al. [48], no data are available about using hybrid ZnO and WO_3 with an active solar still system. The present work aims to use nanofluids, to enhance thermal conductivity to raise the efficiency of a solar collector. Hence, hotter water entered the solar still through the heat exchanger. Consequently, more distilled water is produced. Hybrid nanofluids with different percentages of ZnO and WO_3 nanoparticles were prepared. Limited research work was done on hybrid nanofluids, and no work studied hybrid ZnO with WO_3 nanoparticles although it is the new trend using nanofluid as reviewed by Tiwari et al. [49], Salman et al. [50], Hu et al. [51], and Sundar et al. [52]. ZnO nanoparticles were selected as it has higher thermal conductivity, while WO_3 nanoparticles were used as it has good stability, as Sharafeldin et al. [53].

The present study aims to identify an appropriate preparation technique for producing a stable hybrid nanofluid. One of the original parts of our study is the estimation of the thermal conductivity of a hybrid ZnO + WO_3/water nanofluid. Subsequently, it is imperative to evaluate the effectiveness of the solar collector using mono and hybrid (ZnO and WO_3)/water nanofluids to validate the practicality of the research findings. The solar still productivity is a key focus of the current study. Therefore, productivity will be demonstrated to emphasize the significance of the ongoing effort, which

Table 1 Hybrid nanoparticles volume fraction

Cases	Volume fraction ratio of ZnO %	Volume fraction ratio of WO_3%	Water/Liter	Total volume fraction/%
Case 1	0.035	–	2	0.035
Case 2	0.025	0.01	2	0.035
Case 3	0.02	0.015	2	0.035
Case 4	0.015	0.02	2	0.035
Case 5	0.01	0.025	2	0.035
Case 6	–	0.035	2	0.035

Table 2 zeta potential for hybrid ZnO-WO_3/ water nanofluid

Cases	The volume fraction ratio of ZnO %	The volume fraction ratio of WO_3%	Zeta potential/mV
Case 1	0.035	–	−41.99
Case 2	0.025	0.01%	−30.91
Case 3	0.02	0.015%	−34.97
Case 4	0.015	0.02%	−35.36
Case 5	0.01	0.025%	−39.15
Case 6	–	0.035%	−40.68

encourages enterprises and governments to invest in the existing concept for increased production of clean water.

Hybrid nanofluid

Preparation methods

Nanofluid was prepared with a two-step method. In the first step, nanoparticles were created by MK (Impex, Canada) company as powder. Then, the powder of nanoparticles was synthesized with distilled water. Two different nanoparticles were chosen in the presented work, ZnO and WO_3. The diameter of ZnO was 30 nm, while it was 90 nm for WO_3. Nanoparticles were weighted using a balance that had a step of 1 mg. The amount of nanoparticles was chosen to achieve the needed volume concentration, which is shown in Table 1. After that, nanoparticle powder was mixed with two liters of water by an ultrasonic probe (Hielscher, UP200S), with a maximum output of 200 W. The duration of the mixing process was one hour. Ultrasonic waves were used to disrupt the aggregation of hybrid nanoparticles, facilitating their dispersion within the aqueous medium. The instances under investigation are shown in Table 1, with Case 1 representing the mono ZnO/water nanofluid and Case 6 representing the mono WO_3/water nanofluid. Case 2,3,4,5 was the case of hybrid ZnO + WO_3 nanoparticles with different volume concentrations. The main concept in the presented work is studying the same total volume fraction of 0.035% for all cases, and the difference between cases is the partial volume fraction for each nanoparticle. The summation of the volume fraction of ZnO nanoparticles with the corresponding concentration of WO_3 for any case must be 0.035%. The volume fraction of 0.035% was chosen as it gave acceptable stability in all cases for mono and hybrid nanofluid.

Nanofluid stability

The main problem of the limited use of nanofluids is stability. Stable nanofluid keeps the thermal properties of nanofluid during operation. In the presented work, two methods are used to check the stability. The first test is done using a PALS Zeta potential analyzer (Ver. 3.37 from Brookhaven Instruments). According to Mahbubul et al. [54], if the mean value is less than −30 mV or more than +30 mV, the nanofluid is deemed stable. The mean zeta potential value for nanofluid is shown in Table 2, which shows that mono nanofluid stability (ZnO and WO_3) has higher stability than the hybrid ZnO + WO_3. The mean zeta potential value for ZnO 0.025% + WO_3 0.01% is −30.91mV, while for ZnO 0.01% + WO_3 0.025% −39.15mV. For ZnO 0.02% + WO_3 0.015% and ZnO 0.015% + WO_3 0.02%, values are −34.97 mV and −35.36 mV, respectively. These results indicated that the mono nanofluid of ZnO and WO_3 is more stable than the hybrid nanofluid. However, making a hybrid nanofluid of ZnO and WO_3 can be achieved for a concentration of 0.035%. Converging proportions of ZnO and WO_3 have less stability compared with divergent proportions. Another checking method was done by eye check, where the mixture of nanoparticles and water was observed for 72 h. During that period, no free surface appeared, which means that the hybrid ZnO and WO_3 are stable and applicable for the presented work where a pump is circulating the nanofluid. Figure 1 shows the nanofluids when they were freshly made and after 72 h of preparation.

Thermal conductivity

The primary goal of incorporating nanoparticles into base fluids is to enhance thermal conductivity. Many studies have been conducted to demonstrate the thermal conductivity of nanofluids. Their research discovered that the value of nanofluids varies depending on their kind, concentration, and temperature. Based on this, one of the innovative aspects of our study is the determination of the thermal conductivity of a hybrid ZnO + WO_3/water nanofluid. Measurements were taken using a thermal conductivity tester type SKZ1061C TPS. Its measuring range is 0.005—300 W m^{-1} K^{-1} with 5% accuracy. The testing time is about 5–160 s according to the manufacturer while in the presented study the reading is taken after 2 min while it reaches steady results. It measures temperatures

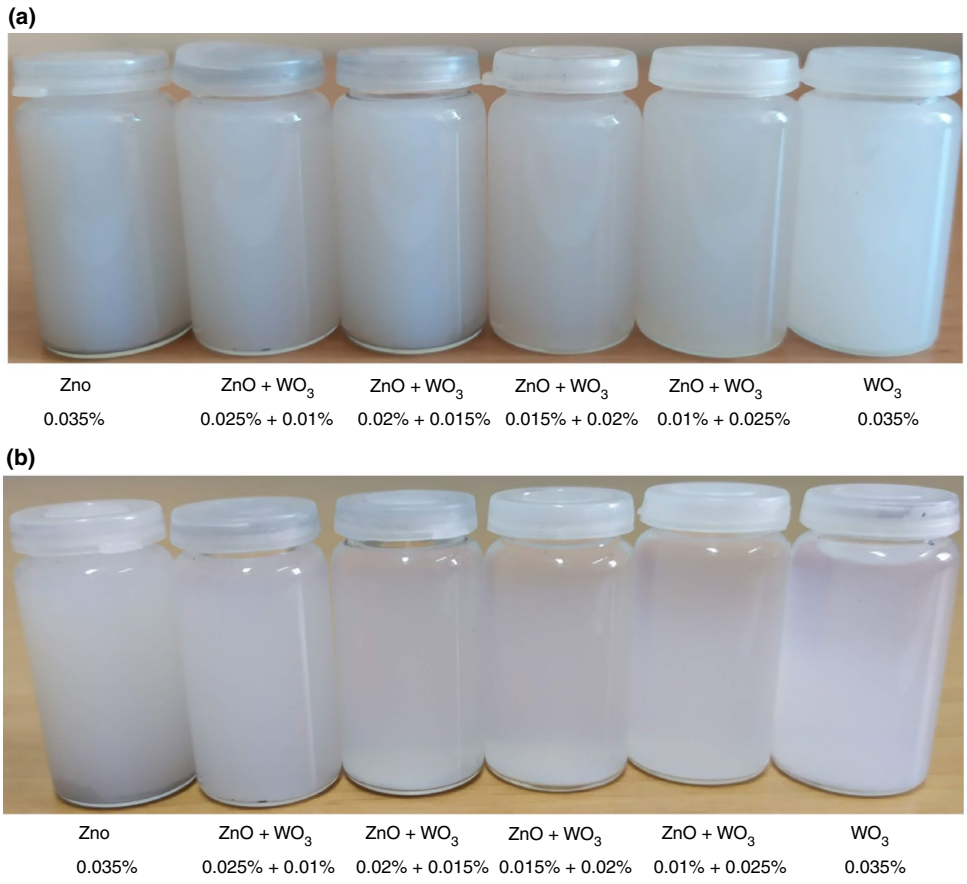

Fig. 1 Photos for the prepared nanofluids **a** freshly prepared **b** after 72 h

from ambient to 130°C, which is appropriate for the present research. Its technique of operation is to heat a planar sensor by applying an electrical current under transitory situations. The sensor temperature changes with time are then established, and when the voltage and electrical resistance of the sensor change, thermal conductivity may be supplied.

Experimental test rig

The present work aims to investigate the performance of active solar still with a heat exchanger. Hence, the main components are the solar collector, pump, heat exchanger, and solar still. Figure 2a depicts the test rig's components while Fig. 2b shows the real photo of used components. The main components of the system are a solar collector, solar still, collecting bottle, heat exchanger, valve, pump, flow meter, and thermometer. Table 3 indicates the solar collector's necessary features. The solar still is double slope one. A heat exchanger is integrated into the bottom of the solar still. The system operates by circulating nanofluids in a closed loop via a pump. During the circulation, nanofluids enter the solar collector, where their temperature increases. In the solar still, only heat from nanofluids is transferred to the basin water. The proposed study investigates how heat from nanofluids contributes to increased productivity in solar stills. Pt-100 resistance, a flow meter, a weather station, and a flask are used for collecting data. Thermometers monitor the temperature of the fluid at its input and output. The flow meter is used to measure the flow rate of nanofluids.

Mathematical equations

The thermodynamics first law is used to accomplish performance analysis. Equation (1) calculates the beneficial heat gain.

$$Q_u = \dot{m}C_p\left(T_o - T_i\right) = \rho V \cdot C_p\left(T_o - T_i\right) \tag{1}$$

This equation is made by measuring the flow rates and temperatures. According to the standard, the beneficial heat gain is computed as the difference between solar energy absorbed and the lost heat energy as Eq. (2).

$$Q_u = A_c F_R\left[G_T(\tau\alpha) - U_L\left(T_i - T_a\right)\right] \tag{2}$$

Then, the instantaneous efficiency, known as the Hottel-Whillier equation, is estimated based on Eq. (3).

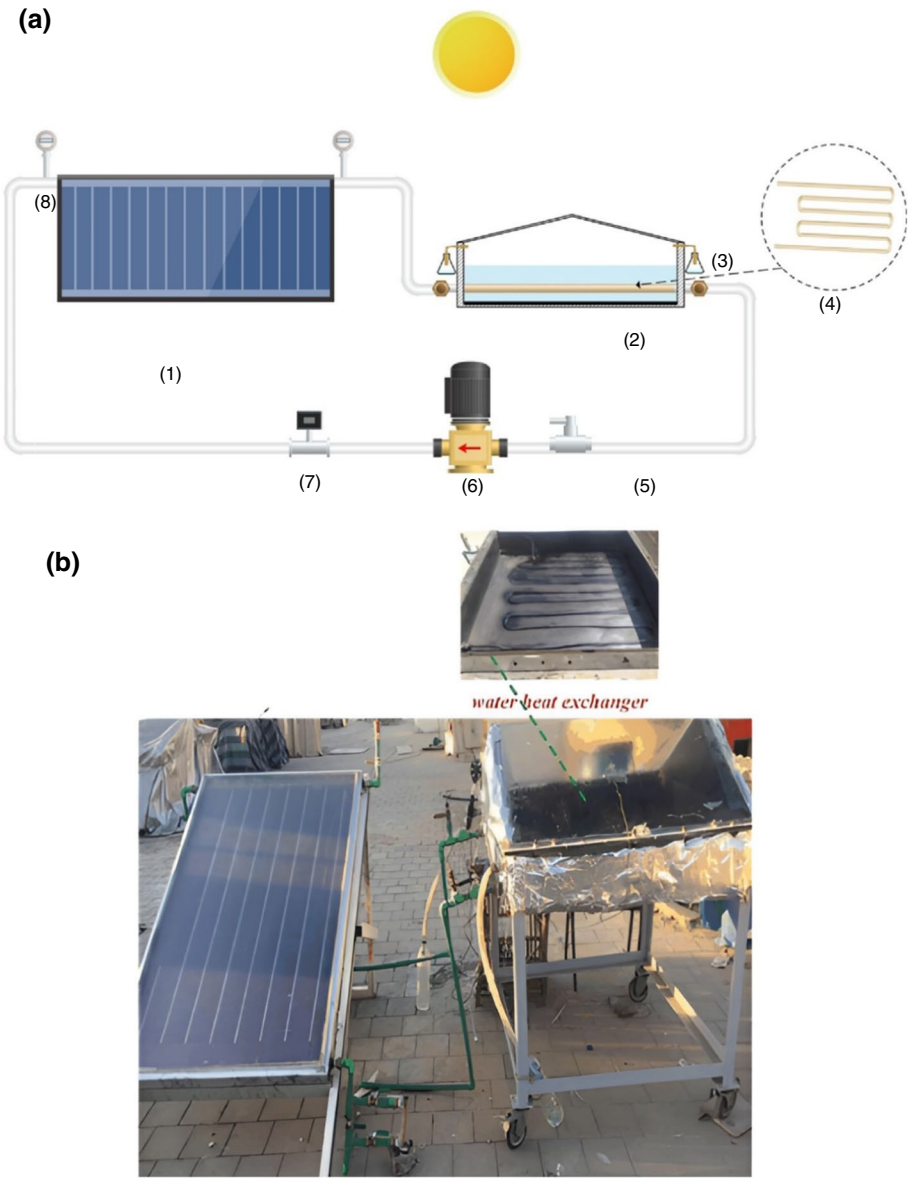

Fig. 2 **a** Shows the test rig components (1) solar collector (2) solar still (3) collecting bottle (4) heat exchanger (5) valve (6) pump (7) flow meter (8) thermometer. **b** photo for the tested system

Table 3 Features of the solar collector

Specification	Dimension
Width	796 mm
Length	2005 mm
Height	136 mm
Absorber absorption coefficient	0.93
Absorber emission factor	0.08
Gross area	1.59 m^2
Aperture area	0.8, m^2
Liquid space capacity	0.31, liter
Thermal insulation thickness and material	Average > 50mm glass wool

$$\eta_i = \frac{\rho V \cdot C_p (T_o - T_i)}{A_c G_T} = \frac{A_c F_R \left[G_T(\tau\alpha) - U_L (T_i - T_a) \right]}{A_c G_T} = F_R (\tau\alpha) - F_R U_L \left(\frac{T_i - T_a}{G_T} \right) \quad (3)$$

The heat removal factor is calculated using the following equation,

$$F_R = \frac{\dot{m} C_p (T_o - T_i)}{A_c \left[G_T(\tau\alpha) - U_L (T_i - T_a) \right]} \quad (4)$$

An array of solar collectors was employed to heat the nanofluids. Thus, the solar radiation on the solar collectors

and the electricity used by the pump should also be included when estimating the total efficiency of a solar still. Furthermore, Pump power is included in the entire solar still efficiency, which is expressed as [26].

$$\eta_{\text{overall}} = \frac{\sum \dot{m}_{\text{ew}} * h_{\text{fg}}}{(\sum G_{\text{T}} * A_{\text{s}}) + \sum G_{\text{T}} * A_{\text{s}}) + \text{pump power}} \quad (5)$$

Water vapor latent heat, which is presumed, on average, in the temperature range, of 2325 kJ/(kg).

The ratio of solar still overall efficiency enhancement

$$= \frac{\eta_{\text{overall(nanofluid)}} - \eta_{\text{overall(water)}}}{\eta_{\text{overall(water)}}} * 100\% \quad (6)$$

The density and specific heat of the hybrid nanofluid can be calculated as Eqs. (7) and (8)

$$\rho_{\text{nf}} = \rho_{\text{np1}}(\varphi_1) + \rho_{\text{np2}}(\varphi_2) + \rho_{\text{bf}}(1 - \varphi_1 - \varphi_2) \quad (7)$$

$$(\rho C_{\text{p}})_{\text{nf}} = (\rho C_{\text{p}})_{\text{np1}}(\varphi_1) + (\rho C_{\text{p}})_{\text{np2}}(\varphi_2) + (\rho C_{\text{bf}})_{\text{bf}}(1 - \varphi_1 - \varphi_2) \quad (8)$$

Results

5.1. Thermal conductivity

Using nanoparticles is primarily motivated by their excellent heat conductivity. When compared to water, ZnO and WO_3 have higher heat conductivity. The % increase in thermal conductivity for nanofluid is shown in Figure 3. The ratio of the thermal conductivity enhancement is determined using equation (11) in the following manner:

$$\text{Enhacement in thermal codactuvity} = \frac{k_{\text{nf}} - k_{\text{bf}}}{k_{\text{bf}}} * 100\% \quad (9)$$

The enhancement ratio for mono nanofluid ZnO with 0.035% volume fraction increases by 5.65% to 9.46%, 13.27%, 17.09%, 20.93%, and 24.8% for temperatures of 30, 35, 40, 45, 50, 55 °C, respectively. Mono WO_3 nanofluid with a concentration of 0.035% thermal conductivity reaches a rise of 5.18%, 6.59%, 8.05%, 9.57%, 11.15%, and 12.8% compared with water for temperatures of 30, 35, 40, 45, 50, 55 °C, respectively. For hybrid nanofluid case 2 where ZnO and WO_3 concentration are 0.025%, and 0.01%, respectively thermal conductivity excess by 5.62%, 8.88%, 12.06%, 15.27%, 18.5%, and 21.78% for temperatures of 30, 35, 40, 45, 50, 55 °C When ZnO concentration was decreased to 0.02% in case 3 the values dropped to 5.6%, 8.53%, 11%, 13.51%, 16.06%, and 18.67%. Although WO_3 concentration increases to 0.02% in case 4, thermal conductivity only gets up by 5.34%, 7.79%, 10.27%, 12.79%, 15.35%, and 17.96% for temperatures of 30, 35, 40, 45, 50, 55 °C, respectively. More increase in WO_3 concentration to be 0.025% in case 5 facing more declining the enhancement ratio to be 5.25%, 7.29%, 9.38%, 11.52%, 13.7%, and 15.5% for temperatures of 30, 35, 40, 45, 50, 55 °C, respectively.

These results of thermal conductivity enhancement revealed that the thermal conductivity of nanofluid is superior to water. More thermal conductivity is found if ZnO nanoparticles are used compared with WO_3 nanoparticles at the same concentration. For hybrid nanofluid (ZnO and WO_3), as the ratio of ZnO concentration in the hybrid

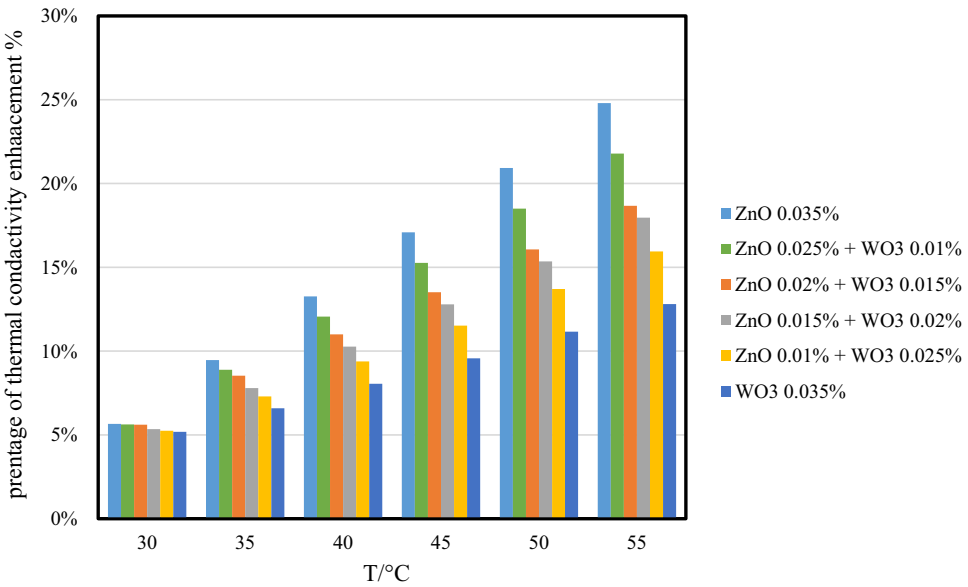

Fig. 3 The increasing percentage of thermal conductivity of nanofluid at different temperatures

nanofluid increases, the thermal conductivity increases. The maximum thermal conductivity was measured for case 2, where the concertation of ZnO and WO_3 is 0.025% and 0.01%, respectively. Less value is found for case 3, where the concertation of ZnO and WO_3 is 0.02% and 0.015%, respectively, but it is still above the value of case 4 with concertation of ZnO and WO_3 is 0.015% and 0.02%, respectively. The lowest value of hybrid nanofluid detected in the presented work is for case 5, with the concentration of ZnO and WO_3 being 0.01% and 0.025%, respectively. The reason for that is that ZnO nanoparticles have higher thermal conductivity compared with WO_3. Free electrons for ZnO are more than WO_3. Hence, these electrons help to work as a bridge to transfer more heat energy. The number of it can be increased with the increase of ZnO nanoparticles in the hybrid solution.

5.2. Collector thermal efficiency

One of the main results expressed in the presented study is the collector thermal efficiency of the collector. Collector thermal efficiency is computed instantaneously. Equation (3) is used to make the calculation. ASHRAE Standard 93–2003 is the typical on which the analysis was made based on. The standard expressed that collector thermal efficiency is the ratio between the thermal energy absorbed by the collector and the existing solar energy. Throughout work, collector thermal efficiency for different concentrations of water, mono, and hybrid (ZnO and WO_3) were checked at different volume flow rates. Concentrations of ZnO and WO_3 were expressed in Table 2. Volume flow rates examined in the presented work are 0.042, 0.052, and 0.062 m^{-3} h^{-1}. The relation between collector thermal instantaneous efficiency and the reduced temperature parameter [(Ti–Ta)/GT] can be fitted in a linear curve. The maximum value of efficiency appeared when the fitted curve intersected with the Y-axis and is known as the thermal optical efficiency, which has the abbreviation of $\boldsymbol{F_R}$ $(\boldsymbol{\tau\alpha})$. The slope of the fitted curve is known as the energy removal parameter and has an abbreviation of $\boldsymbol{F_R U_L}$. Values of $\boldsymbol{F_R}$ $(\boldsymbol{\tau\alpha})$ and $\boldsymbol{F_R U_L}$ for different nanofluid concentrations at different volume flow rates are shown in Table 4. The methodology of studying hybrid nanofluid in the current work is based on analyzing the same volume concentration of two different nanoparticles (ZnO and WO_3) where, in any case, the total volume fraction is 0.035% and from one case to another, the percentage of each nanoparticle changes. Also, cases of mono nanoparticles of (ZnO and WO_3) are studied for the same volume concentration of 0.035%. Water as the base fluid case was tested. Based on the presented cases, the results for mono and hybrid nanofluid are presented, and the effect of mixing ZnO and WO_3 nanoparticles is shown. The comparison of results for different mixing percentages of ZnO and WO_3 helps to identify the best working condition for each case. These results support reads to judge the suitable percentage of mixing of ZnO and WO_3 according to the application where nanofluids are used.

Table 4 Values of $\boldsymbol{F_R}$ $(\boldsymbol{\tau\alpha})$ and $\boldsymbol{F_R U_L}$ for different nanofluid and different volume flow rates.

Volume flow rate/ m^{-3} h^{-1}	Case	fluid	$F_R/\tau\alpha$	$F_R U_L$	R^2
0.042		Water	0.39	3.82	0.98
	Case 1	ZnO 0.035%	0.62	26.07	0.99
	Case 2	ZnO 0.025% + WO_3 0.01%	0.60	24.85	0.98
	Case 3	ZnO 0.02% + WO_3 0.015%	0.58	23.27	0.99
	Case 4	ZnO 0.015% + WO_3 0.02%	0.56	20.91	0.98
	Case 5	ZnO 0.01% + WO_3 0.025%	0.53	17.55	0.98
	Case 6	WO_3 0.035%	0.48	13.59	0.99
0.052		Water	0.4	4.85	0.98
	Case 1	ZnO 0.035%	0.68	34.26	0.97
	Case 2	ZnO 0.025% + WO_3 0.01%	0.65	30.35	0.98
	Case 3	ZnO 0.02% + WO_3 0.015%	0.63	29.3	0.97
	Case 4	ZnO 0.015% + WO_3 0.02%	0.59	26.2	0.97
	Case 5	ZnO 0.01% + WO_3 0.025%	0.55	21.72	0.98
	Case 6	WO_3 0.035%	0.51	17.77	0.98
0.062		Water	0.41	5.48	0.98
	Case 1	ZnO 0.035%	0.71	34.89	0.97
	Case 2	ZnO 0.025% + WO_3 0.01%	0.68	34.04	0.99
	Case 3	ZnO 0.02% + WO_3 0.015%	0.66	32.32	0.99
	Case 4	ZnO 0.015% + WO_3 0.02%	0.61	29.28	0.98
	Case 5	ZnO 0.01% + WO_3 0.025%	0.57	26.33	0.98
	Case 6	WO_3 0.035%	0.52	21.11	0.99

Figure 4 shows the relation between collector thermal instantaneous efficiency and the reduced temperature parameter $[(T_i–T_a)/G_T]$ for different concentrations of hybrid nanofluid of (ZnO and WO_3) and water. Figure 4 is drawn for the volume flow rate of 0.042 m^{-3} h^{-1}. Based on Fig. 4 $\boldsymbol{F_R}$ $(\boldsymbol{\tau\alpha})$ and $\boldsymbol{F_R U_L}$ values for water are 0.39 and − 3.82, respectively. For mono nanofluids ZnO values for $\boldsymbol{F_R}$ $(\boldsymbol{\tau\alpha})$ and $\boldsymbol{F_R U_L}$ are 0.62, and 26.07 while WO_3 values are 0.48 and 13.59, respectively. Hybrid nanofluids of ZnO and WO_3 have values

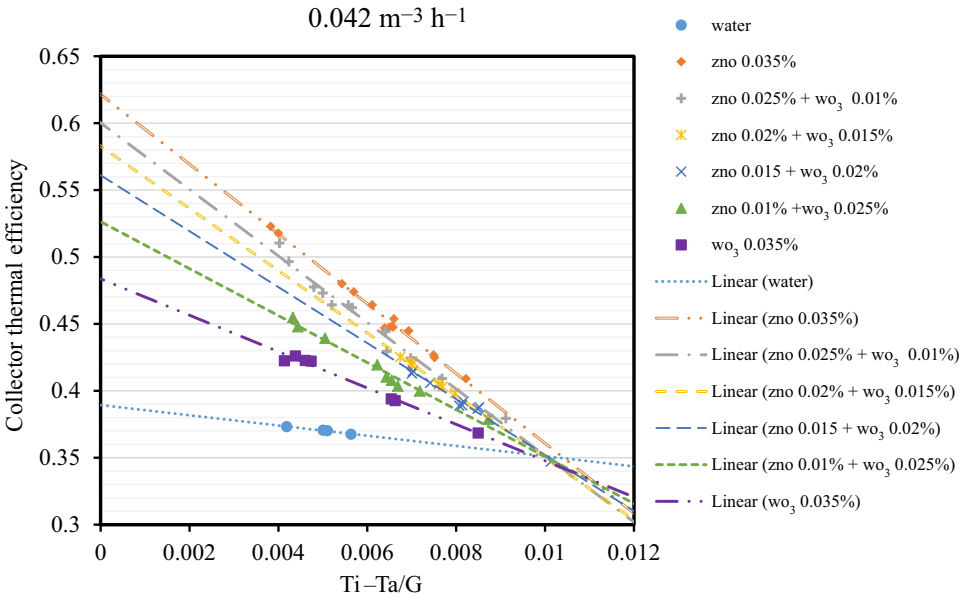

Fig. 4 Collector thermal efficiency in the case of water and nanofluid for the volume flow rate of 0.042 m^{-3} h^{-1}

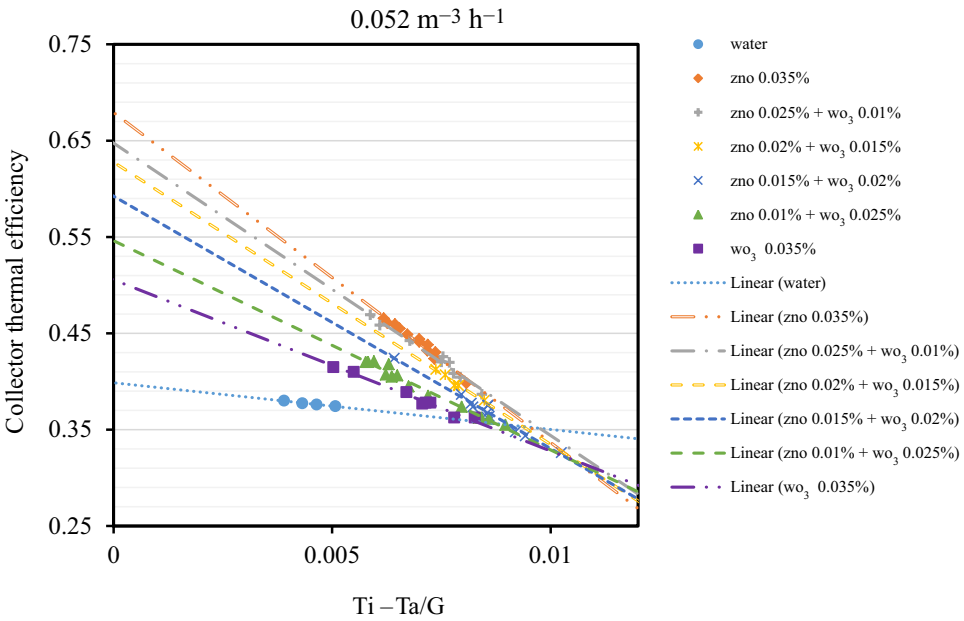

Fig. 5 Collector thermal efficiency in the case of water and nanofluid for the volume flow rate of 0.052 m^{-3} h^{-1}

of 0.60 and 24.85, 0.58 and 23.27, 0.56 and 20.91, 0.53 and 17.55 for cases 2, 3, 4, and 5, respectively.

Figure 5 expresses the collector thermal efficiency of the solar collector when the volume flow rate is 0.052 m^{-3} h^{-1}. Results are shown for water and mono nanofluid of ZnO and WO_3. Also, different concentrations of hybrid ZnO and WO_3 are tested at 0.052 m^{-3} h^{-1}. Thermal optical efficiency $\mathbf{F_R}$ $(\boldsymbol{\tau\alpha})$ increased from 0.4 for water to 0.51 and 0.68 for mono nanofluid WO_3 and ZnO, respectively. But the energy removal parameter $\boldsymbol{F_R U_L}$ went up from 4.85 to 34.26 and 17.77 for mono nanofluid WO_3 and ZnO, respectively. Hybrid nanofluid results indicated that and $\boldsymbol{F_R}$ $(\boldsymbol{\tau\alpha})$ values enhanced from 0.55 to 0.59, 0.63, and 0.65 for cases 5, 4, 3, and 2, respectively. In addition, values for $\boldsymbol{F_R U_L}$ change from 21.72, 26.2, 29.3, and 30.35 for cases 5, 4, 3, and 2, respectively.

The maximum volume flow rate used in the presented work is 0.62 m^{-3} h^{-1}, as shown in Fig. 6. Water, mono nanofluid, and hybrid nanofluid were examined at that volume flow rate. It was found that the thermal optical efficiency is 0.41 for water, 0.71 for ZnO, and 0.52 for water. Besides that, the energy removal parameter is 5.48 for water, 34.89 for ZnO, and 21.11 for WO_3. Case 2 values for the thermal optical efficiency and the energy removal parameter are

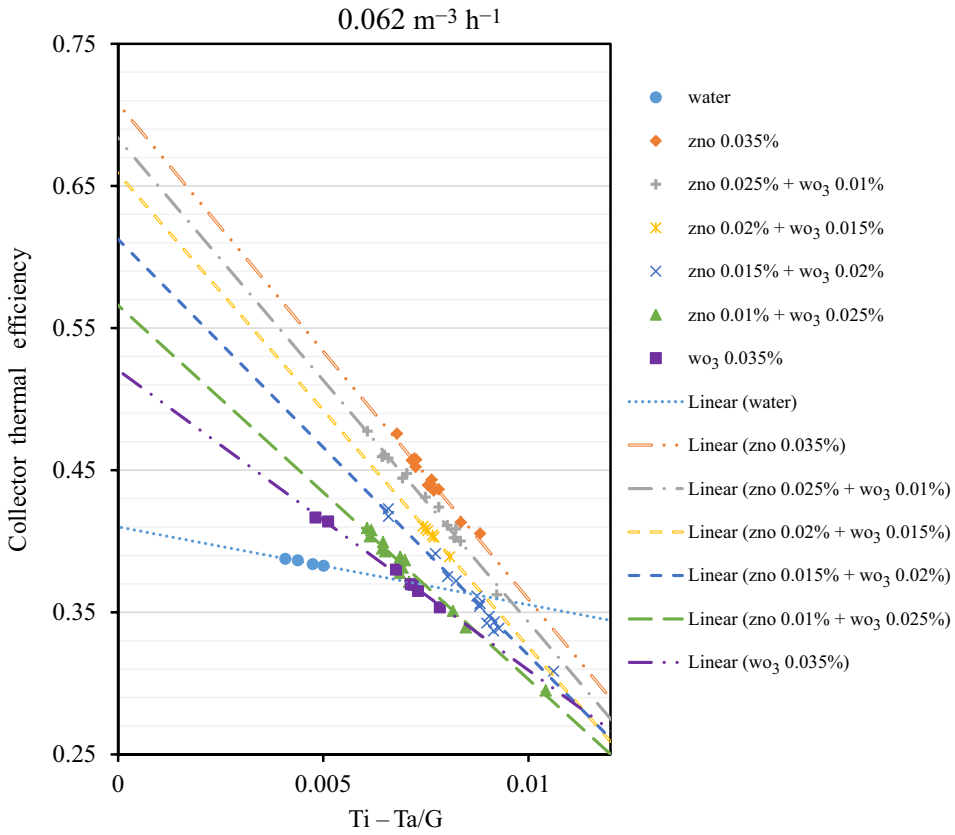

Fig. 6 Collector thermal efficiency in the case of water and nanofluid for the volume flow rate of 0.062 m^{-3} h^{-1}

0.683 and 34.04, respectively. While for case 3, the values are 0.66 and 32.32. Fewer values are found for case 4 to be 0.61 and 29.28. lower values are given to case 5 to be 0.57 and 26.33.

The water, mono, and hybrid nanofluid collector thermal efficiency curves for the solar collector employed in the study presented are shown in Figs. 4, 5, and 6, as well as Table 4. The greatest efficiency of the collector occurs when the ambient temperature Ta and the fluid temperature Ti are identical, which is known as thermal optical efficiency $\boldsymbol{F_R}$ $(\boldsymbol{\tau\alpha})$. The energy removal parameter $\boldsymbol{F_R}$ $\boldsymbol{U_L}$, which relates to thermal energy loss, is represented by the slope of the fitted curve. The study given adheres to ASHRAE Standard 93–2003, which establishes that when the decreased temperature parameter $[(T_i–T_a)/G_T]$ increases, solar collector efficiency drops. It was discovered during our research that nanofluids had a better thermal optical efficiency $\boldsymbol{F_R}$ $(\boldsymbol{\tau\alpha})$ than water. ZnO with a concentration of 0.035% has more thermal optical efficiency $\boldsymbol{F_R}$ $(\boldsymbol{\tau\alpha})$ compared with WO_3 with the same concentration. Hybrid nanofluids of ZnO and WO_3 have a total concentration of 0.035% but have different percentages of particles. It was found that as the percentage of ZnO increases the thermal optical efficiency rises and vice versa. The energy removal parameter $\boldsymbol{F_R}$ $\boldsymbol{U_L}$ which refers to heat energy lost being higher for nanofluids compared with water. Less heat energy is lost in the case of WO_3 compared with ZnO. For hybrid ZnO and WO_3, as the percentage of ZnO decreases, the heat energy lost declines. The reason for that way is thermal conductivity. Thermal conductivity is explained in Fig. 3. As thermal conductivity increases both thermal optical efficiency $\boldsymbol{F_R}$ $(\boldsymbol{\tau\alpha})$ and energy removal parameter $\boldsymbol{F_R}$ $\boldsymbol{U_L}$ increased. Based on that, more energy can be transmitted from the absorber plate of the collector to the moving fluid. Hence more useful heat energy is absorbed, and higher thermal efficiency is achieved.

5.3. Heat removal factor

Calculating the heat removal factor is another technique to study the influence of hybrid nanofluid on the performance of solar collectors. The heat removal factor is defined as the ratio of heat energy absorbed by the collector to the heat energy available. It is regarded as a real measure of the return on investment from the usage of hybrid nanofluids in solar energy. The usage of nanofluids is encouraged if the heat removal factor rises, and vice versa. Equation (4) may be used to compute the heat removal factor. Figure 7 depicts the heat removal factor for water and various nanofluid concentrations at the examined volume flow rate. Water had values of 0.44, 0.45, and 0.46 at volume flow rates of 0.042, 0.052, and 0.062 m^{-3} h^{-1}, respectively. The most significant values for F_R were 0.7, 0.77, and 0.8 for ZnO mono

nanofluid with a concentration of 0.035% at volume flow rates of 0.042, 0.052, and 0.062 m^{-3} h^{-1}, respectively. The minimum values for WO_3 mono nanofluid with a concentration of 0.035% are 0.55, 0.57, and 0.59 for volume flow rates of 0.042, 0.052, and 0.062 m^{-3} h^{-1}, respectively.

Values for hybrid nanofluids increase from 0.55, 0.60, 0.64, 0.66, to 0.68 for the concentrations of ZnO 0.01% + WO_3 0.025%, ZnO 0.015% + WO_3 0.02%, ZnO 0.02% + WO_3 0.015%, and ZnO 0.025% + WO_3 0.01% for the volume flow rate of 0.042 m^{-3} h^{-1}, respectively. A clear rise is found for the volume flow rate of 0.052 m^{-3} h^{-1}. Values are 0.57, 0.62, 0.67, 0.71, and 0.73 for the concentrations of ZnO 0.01% + WO_3 0.025%, ZnO 0.015% + WO_3 0.02%, ZnO 0.02% + WO_3 0.015%, and ZnO 0.025% + WO_3 0.01%, respectively. Maximum values are 0.59, 0.64, 0.69, 0.75, and 0.77 for the concentrations of ZnO 0.01% + WO_3 0.025%, ZnO 0.015% + WO_3 0.02%, ZnO 0.02% + WO_3 0.015%, and ZnO 0.025% + WO_3 0.01% for the volume flow rate of 0.062 m^{-3} h^{-1}, respectively. Results indicate that using nanofluids heightens the heat removal factor which implies more energy can be absorbed when nanofluids are used. The heat removal factor increases with the rise of the volume flow rate of fluids. Adding more ZnO to the hybrid ZnO + WO_3 nanofluid enhances the heat removal factor. Thermal conductivity is the reason for the rise in heat removal factor.

5.4. Daily distilled water production

The primary goal of desalination research is to produce water. Through the heat exchanger, the heat energy captured by the solar collector is transferred to salty water in the solar still. That heat aids in raising the temperature of salty water and increasing its evaporation rate. Consequently, more distilled water is created. Figure 8 shows the daily quantity of distilled water generated for the various nanofluid containers utilized in the solar collector. For volume flow rates of 0.042, 0.052, and 0.062 m^{-3} h^{-1}, respectively, the highest quantity of water produced by ZnO mono nanofluid is 3.09, 3.11, and 3.14 kg day^{-1} m^{-2}. The minimal values for water are 2.52, 2.68, and 2.75 kg day^{-1} m^{-2} for volume flow rates of 0.042, 0.052, and 0.062 m^{-3} h^{-1}, respectively. Higher values are obtained for WO_3 mono nanofluids at volume flow rates of 0.042, 0.052, and 0.062 m^{-3} h^{-1}, respectively. For hybrid nanofluids, lower values of 2.88, 2.93, and 2.96 kg day^{-1} m^{-2} are achieved for ZnO 0.01% + WO_3 0.025%, while maximum values for ZnO 0.025% + WO_3 0.01% are 3.05, 3.07, and 3.08 kg day^{-1} m^{-2} for volume flow rates of 0.042, 0.052, and 0.062 m^{-3} h^{-1}, respectively. The results for ZnO 0.02% + WO_3 0.015% rise from 2.99 to 3.02 and 3.04 at volume flow rates of 0.042, 0.052, and 0.062 m^{-3} h^{-1}, respectively. The results for ZnO 0.015% + WO_3 0.02% are 2.89, 2.93, and 2.96 kg day^{-1} m^{-2} for volume flow rates of 0.042, 0.052, and 0.062 m^{-3} h^{-1}, respectively. According to the findings, utilizing nanofluid has a beneficial influence on daily distilled water output. Increasing the amount of ZnO nanoparticles in a hybrid nanofluid of ZnO + WO_3 nanofluid improves the amount of distilled water produced. Also, the daily distilled water production increases with the rise of the volume flow rate. The reason for that is thermal conductivity as it rises with the increase in the ZnO ratio in a hybrid nanofluid. Consequently, more heat is absorbed by the collector. Hence, more energy is transferred to salty water, and a higher evaporation ratio is obtained.

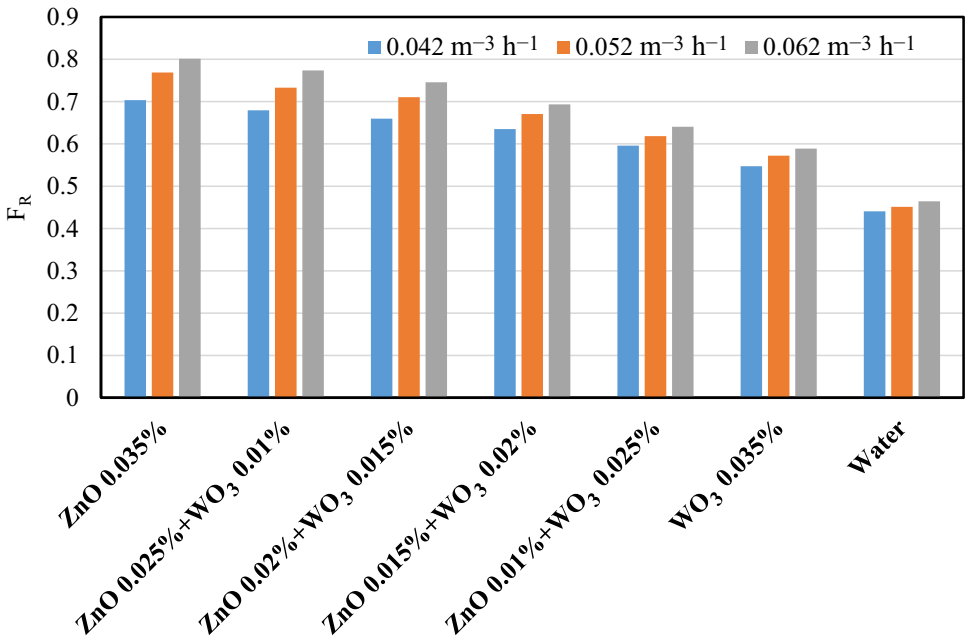

Fig. 7 Heat removal factor for different nanofluids for studied volume flow rates

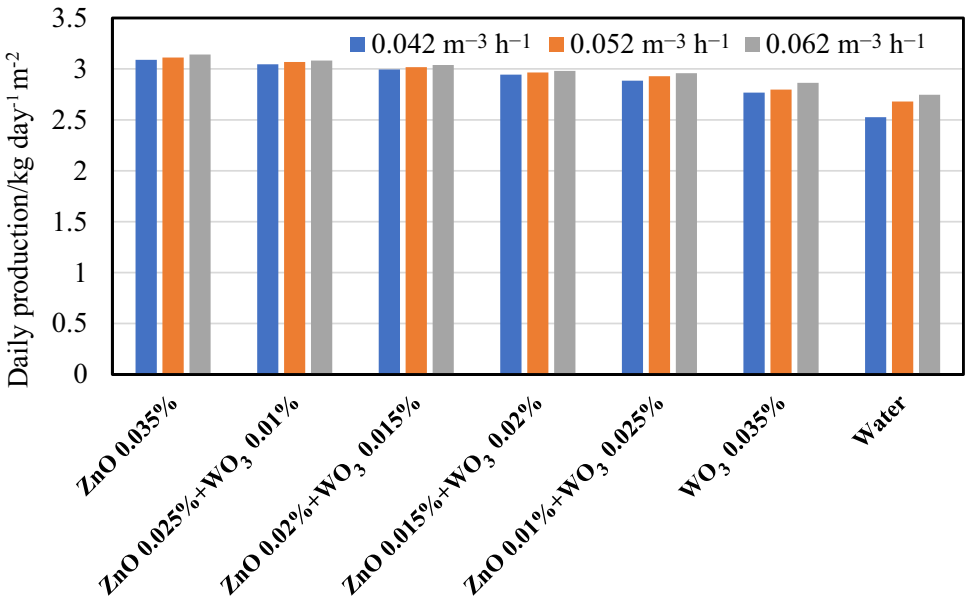

Fig. 8 Daily distilled water production for different nanofluids for studied volume flow rates

5.5. Solar still overall efficiency

Solar still overall efficiency is the ratio between energy contained in the distilled water produced to the sum of solar energy and pump power paid to produce that distilled water. That efficiency is the ratio between what is gained from solar still, which is distilled water, to what is needed to make that water, which is solar energy and pump power. Higher efficiency means more distilled water is produced with less energy consumed by solar energy and pump power. One of the seeks of the existing work is to increase solar still efficiency using nanofluids in the heat exchanger. Overall solar still efficiency is calculated based on Eq. (5) for both water and nanofluids. Figure 9 shows solar still efficiency for water, mono nanoparticles, and hybrid nanofluids. The ratio of enhancement in solar still is presented in Fig. 10. Results indicated that using ZnO nanofluids in the heat exchanger has higher efficiency of 39.4, 39.6, and 39.9 for the volume flow rates of 0.042, 0.052, 0.062 m^{-3} h^{-1}, respectively. The minimum values are 32.2, 34.1, and 34.9 for the volume flow rates of 0.042, 0.052, and 0.062 m^{-3} h^{-1}, respectively, for water. Mono nanofluids of WO_3 have lower values compared with hybrid ZnO + WO_3 nanofluids with values of 35.3, 35.6, and 36.4 for the volume flow rates of 0.042, 0.052, and 0.062 m^{-3} h^{-1}, respectively. For a volume flow rate of 0.042 m^{-3} h^{-1}, values for hybrid nanofluids are 36.8, 37.6, 38.2, and 38.9 for ZnO 0.01% + WO_3 0.025%, ZnO 0.015% + WO_3 0.02%, ZnO 0.02% + WO_3 0.015%, and ZnO 0.025% + WO_3 0.01%, respectively. Higher efficiency values are found for a volume flow rate of 0.052 m^{-3} h^{-1} to be 37.3, 37.8, 38.4, and 39.1 for ZnO 0.01% + WO_3 0.025%, ZnO 0.015% + WO_3 0.02%, ZnO 0.02% + WO_3 0.015%, and ZnO 0.025% + WO_3 0.01%, respectively. The highest values for efficiency are for 0.062 m^{-3} h^{-1} to be 37.6, 37.9, 38.6, and 39.2 for ZnO 0.01% + WO_3 0.025%, ZnO 0.015% + WO_3 0.02%, ZnO 0.02% + WO_3 0.015%, and ZnO 0.025% + WO_3 0.01%, respectively.

Figure 10 shows results for the ratio of enhancement in solar still with nanofluids moving in the heat exchanger. The maximum ratios are for the volume flow rates of 0.042 m^{-3} h^{-1} which are 22.3%, 20.6%, 18.6%, 15.52%, 14.2%, and 9.6% for ZnO 0.035%, ZnO 0.025% + WO_3 0.01%, ZnO 0.02% + WO_3 0.015%, ZnO 0.015% + WO_3 0.02%, ZnO 0.01% + WO_3 0.025%, and WO_3 0.035% respectively. Less ratios are given for 0.052 m^{-3} h^{-1} to be 16.1%, 14.5%, 15.6%, 10.7%, 9.3%, and 4.4% for ZnO 0.035%, ZnO 0.025% + WO_3 0.01%, ZnO 0.02% + WO_3 0.015%, ZnO 0.015% + WO_3 0.02%, ZnO 0.01% + WO_3 0.025%, and WO_3 0.035% respectively. Although 0.062 m^{-3} h^{-1} is the maximum value flow rate used, ratios of enhancement for it are the minimum values to be 14.4%, 12.3%, 10.7%, 8.5%, 7.7%, and 4.3% for ZnO 0.035%, ZnO 0.025% + WO_3 0.01%, ZnO 0.02% + WO_3 0.015%, ZnO 0.015% + WO_3 0.02%, ZnO 0.01% + WO_3 0.025%, and WO_3 0.035% respectively.

Based on Figs. 9 and 10, using nanofluids as the moving fluid in the heat exchanger in the solar still increases its efficiency. Mono nanoparticles of ZnO with a volume concentration of 0.035% gave the maximum values between the studied cases. Lower efficiency values are obtained for WO_3 with a volume concentration of 0.035%. For hybrid nanofluids, the efficiency of solar still became higher with adding more ZnO nanoparticles to the hybrid nanofluids. Solar still efficiency increases with higher volume flow rates of nanofluids. The reason for that is thermal conductivity, which increases with more ZnO nanoparticles added to nanofluids. Hence, more energy

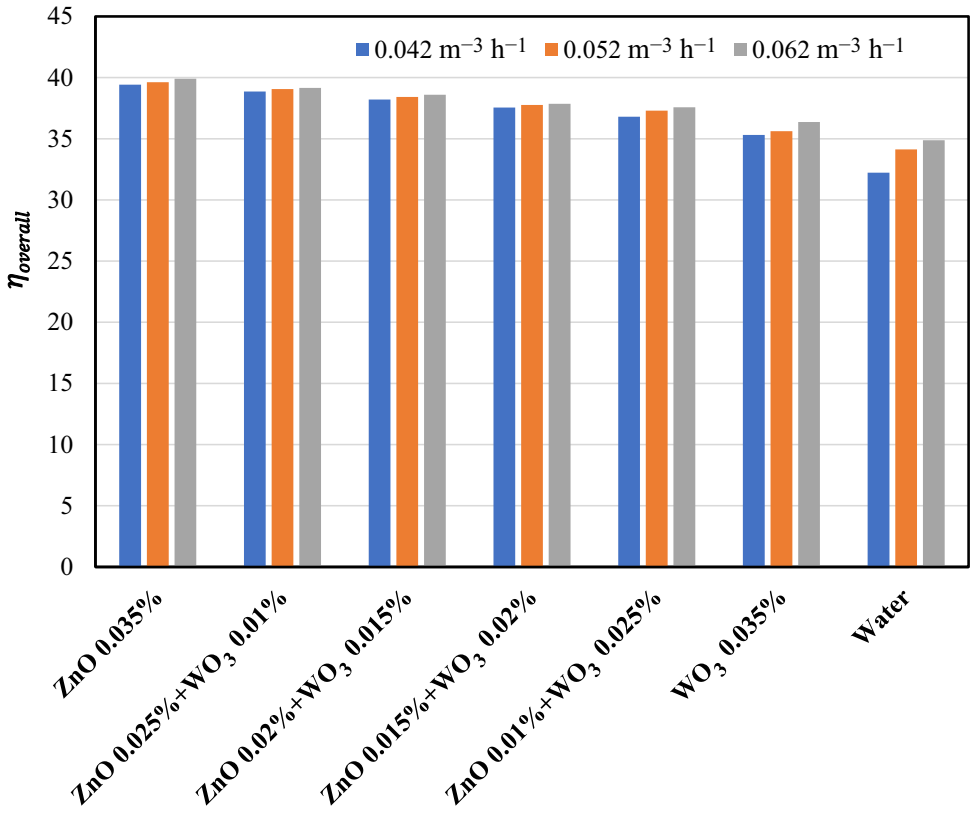

Fig. 9 Solar still overall efficiency included pump power consumption for different nanofluids in the heat exchanger for studied volume flow rates

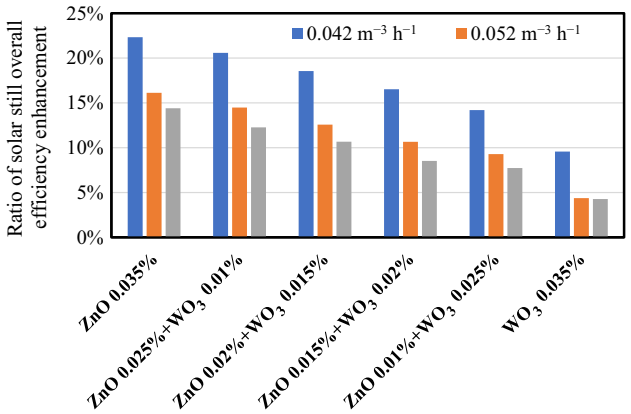

Fig. 10 Ratio of solar still overall efficiency enhancement for different studied volume flow rates

is transferred to saltwater. So more distilled water is brought. However, the ratio of efficiency enhancement of solar still efficiency decreases with the increase of volume flow rates. A lower flow rate means the fluid takes more time to move through the heat exchanger, which allows more heat energy to transfer to salty water. This reason makes more production of distilled water be generated. Hence, a higher ratio of efficiency was achieved.

Conclusions

The current study presents the uses of nanofluids to improve the efficiency of solar stills and collectors. There were six distinct nanofluids made. To create a mono nanofluid, ZnO and WO_3 nanoparticles were combined with water separately. The ZnO and WO_3 mixture was used in four different masses to create hybrid nanofluids. The volume concentration of each nanofluid was 0.035%. It was possible to make nanofluids stable. A heat exchanger was constructed to link a solar still to a solar collector. The solar still's productivity was boosted by nanofluids. When the collector is using a nanofluid and a higher volume flow rate, it can absorb more heat energy. The heat exchanger then transfers more heat energy, enabling the production of more distilled water. Several results were achieved throughout the current work. The following points pointed out the outcomes as follow:

- The thermal conductivity of nanofluids increased between 5.18 and 24.8%.
- ZnO nanoparticles gave the best results, while the lowest values were for WO_3.

- Hybrid ZnO + WO_3 nanofluids indicated moderate values.
- A higher volume flow rate increased the thermal optical efficiency of the collector.
- The heat removal factor showed an increase to 0.8 for ZnO nanofluid, although it was just 0.46 for water at the volume flow rate of 0.62 m^{-3} h^{-1}.
- It was found that as the percentage of ZnO increased in hybrid nanofluid, the distilled water productivity increased.
- A 3.14 kg of distilled water could be produced daily when ZnO/water nanofluid with a concentration of 0.035% was used.
- Solar still overall efficiency, including pump consumption for mono ZnO, reached 39.9%, while for WO_3, it was no more than 36.4%.
- The presented work indicated that a ratio of solar still efficiency enhancement reaches 22.3% in the case of nanofluids compared with water.

Acknowledgments The authors extend their appreciation to the Deputyship for Research & Innovation, Ministry of Education in Saudi Arabia for funding this research work through project number **445-9-478.**

Author contributions Conceptualization was contributed by [Bandar Awadh Almohammadi, Mathkar A. Alharthi],[M. A. Sharafeldin] …; methodology was contributed by [Bandar Awadh Almohammadi, Mathkar A. Alharthi],[M. A. Sharafeldin, Rayed S. Alshareef, Haytham abdelghany] …; formal analysis and investigation were contributed by [M. A. Sharafeldin, Rayed S. Alshareef, Haytham abdelghany], …; writing—original draft preparation, was contributed by [Bandar Awadh Almohammadi, M. A. Sharafeldin, Mathkar A. Alharthi, Mathkar A. Alharthi, Rayed S. Alshareef]; Writing—review and editing, was contributed by [Bandar Awadh Almohammadi, M. A. Sharafeldin, Mathkar A. Alharthi], …; funding acquisition was contributed by [Bandar Awadh Almohammadi, M. A. Sharafeldin, Rayed S. Alshareef], …; resources were contributed by [Bandar Awadh Almohammadi, Mathkar A. Alharthi], …; supervision was contributed by [M. A. Sharafeldin, Mathkar A. Alharthi, Mathkar A. Alharthi, Haytham abdelghany],….

References

1. Rajaseenivasan T, Raja PN, Srithar K. An experimental investigation on a solar still with an integrated flat plate collector. Desalination. 2014;347:131–7.
2. Feilizadeh M, Estahbanati MK, Jafarpur K, Roostaazad R, Feilizadeh M, Taghvaei H. Year-round outdoor experiments on a multi-stage active solar still with different numbers of solar collectors. Appl Energy. 2015;152:39–46.
3. Sharshir SW, Kandeal AW, Algazzar AM, Ayman Eldesoukey MOA, El-Samadony AAH. 4-E analysis of pyramid solar still augmented with external condenser, evacuated tubes, nanofluid and ultrasonic foggers: a comprehensive study. Process Safety Environ Protect. 2022;164:408–17.
4. Sheeba K, Prakash P, Jaisankar S. Performance evaluation of a flat plate collector coupled solar still system. Energy Sources, Part A: Recov Utilization Environ Effects. 2015;37(3):291–8.
5. Manokar AM, Vimala M, Sathyamurthy R, Kabeel A, Winston DP, Chamkha AJ. Enhancement of potable water production from an inclined photovoltaic panel absorber solar still by integrating with flat-plate collector. Environ Dev Sustain. 2020;22(5):4145–67.
6. Al-Molhem YA, Eltawil MA. Enhancing the double-slope solar still performance using simple solar collector and floatable black wicks. Environ Sci Pollut Res. 2020;27(28):35078–98.
7. Abdullah AS, Hadj-Taieb L, Bacha HB, et al. Impact of using sand beds and reflectors on trays solar still performance. J Therm Anal Calorim. 2023;148:10217–26.
8. Shaikh JS, Ismail S. Theoretical investigation on humidification–dehumidification desalination employing flat-plate solar water collector. J Therm Anal Calorim. 2023;148:11835–53.
9. Bafakeeh OT, Shiba MS, Elshalakany AB, et al. Effect of dispersion hybrid structural properties of MWCNTs and Al_2O_3 on microstructural and thermal characteristics of PCMs for thermal energy storage in solar water desalination. J Therm Anal Calorim. 2023;148:4087–104.
10. Menon GS. Parametric factors affecting the performance improvement of a solar still coupled with a flat plate collector. Int J Eng Res. 2016;5(1):30–3.
11. Lalitha Narayana R, Ramachandra Raju V. Effect of flat plate collectors in parallel on the performance of the active solar still for Indian coastal climatic conditions. Int J Ambient Energy. 2019;40(2):203–11.
12. Abdullah AS, Hadj-Taieb L, Mutabe Aljaghtham M, Omara ZM, Essa FA. Enhancing rotating wick solar still performance with various porous breathable belt designs and nanofluid. Case Studies Therm Eng. 2023;49:103205.
13. Maatki C. Heat transfer enhancement using CNT-water nanofluids and two stages of seawater supply in the triangular solar still. Case Studies Therm Eng. 2022;30:101753.
14. Soliman, H., H. Elgohary, M.A. Elmagd, and S. Chowdhury. Brackish water desalination using solar still with built-in heat exchanger coupled to solar collector. In: 2018 IEEE PES/IAS PowerAfrica. 2018. IEEE.
15. Kamarul Baharin ZA, Mohammad MH. Experimental investigations on the performance of a single slope solar still coupled with flat plate solar collector under Malaysian conditions. J Mech Eng (JMechE). 2018;6:16–24.
16. Parsa SM, Norouzpour F, Shoeibi S, Amin Shahsavar S, Said AZ, Guo W. A comprehensive study to find the optimal fraction of nanoparticle coated at the interface of solar desalination absorbers: 5E and GHGs analysis in different seasons. Sol Energy Mater Sol Cells. 2023;256:112308.
17. Balamurugan S, Sundaram NS, Marimuthu KP, Devaraj J. A comparative analysis and effect of water depth on the performance of single slope basin type passive solar still coupled with flat plate collector and evacuated tube collector. Appl Mech Mater. 2017;867:195–202.
18. Shoeibi S, Kargarsharifabad H, Rahbar N. Effects of nano-enhanced phase change material and nano-coated on the performance of solar stills. J Energy Storage. 2021;42: 103061.
19. Abu-Arabi M, Al-harahsheh M, Mousa H, Alzghoul Z. Theoretical investigation of solar desalination with solar still having phase change material and connected to a solar collector. Desalination. 2018;448:60–8.
20. Rai S, Tiwari G. Single basin solar still coupled with flat plate collector. Energy Convers Manage. 1983;23(3):145–9.
21. Morad M, El-Maghawry HA, Wasfy KI. Improving the double slope solar still performance by using flat-plate solar collector and cooling glass cover. Desalination. 2015;373:1–9.
22. Jathar LD, Ganesan S, Shahapurkar K, Soudagar ME, Mujtaba MA, Anqi AE, Farooq M, Khidmatgar A, Goodarzi M, Safaei MR. Effect of various factors and diverse approaches to enhance

the performance of solar stills: a comprehensive review. J Therm Anal Calorim. 2022;147(7):4491–522. https://doi.org/10.1007/s10973-021-10826-y.
23. Sharshir SW, Kandeal AW, Ismail M, Abdelazize GB, Kabeel AE, Yang N. Augmentation of a pyramid solar still performance using evacuated tubes and nanofluid: Experimental approach. Appl Thermal Eng. 2019;160:113997.
24. Saleh SM, Soliman AM, Sharaf MA, Kaled V, Gadgil B. Influence of solvent in the synthesis of nano-structured ZnO by hydrothermal method and their application in solar-still. J Environ Chem Eng. 2017;5:1219–26.
25. Elango T, Kannan A, Kalidasa Murugavel K. Performance study on single basin single slope solar still with different water nanofluids. Desalination. 2015;360:45–51.
26. Kabeel AE, Omara ZM, Essa FA. Enhancement of modified solar still integrated with external condenser using nanofluids: An experimental approach. Energy Convers Manage. 2014;78:493–8.
27. El-Gazar EF, Zahra WK, Hassan H, Rabia SI. Fractional modeling for enhancing the thermal performance of conventional solar still using hybrid nanofluid: energy and exergy analysis. Desalination. 2021;503:114847.
28. Kandeal AW, El-Shafai NM, Abdo MR, Thakur AK, El-Mehasseb IM, Maher I, Maher Rashad AE, Kabeel NY, Sharshir SW. Improved thermo-economic performance of solar desalination via copper chips, nanofluid, and nano-based phase change material. Sol Energy. 2021;224:1313–25.
29. Mahian O, Kianifar A, Heris SZ, Wen D, Sahin AZ, Wongwises S. Nanofluids effects on the evaporation rate in a solar still equipped with a heat exchanger. Nano Energy. 2017;36:134–55.
30. Subhedar DG, Chauhan KV, Patel K, Ramani BM. Performance improvement of a conventional single slope single basin passive solar still by integrating with nanofluid-based parabolic trough collector: An experimental study. Mater Today: Proc. 2020;26:1478–81.
31. El-Ghetany HH, Elgohary HM, Mohammed YM. Performance improvement of solar water distillation system using nanofluid particles. Egypt J Chem. 2021;64(8):4425–31.
32. Akilu S, Baheta AT, Mior AM, Said AA, Minea KVS. Properties of glycerol and ethylene glycol mixture based SiO_2-CuO/C hybrid nanofluid for enhanced solar energy transport. Sol Energy Mater Sol Cells. 2018;179:118–28.
33. Sadeghi G, Nazari S. Retrofitting a thermoelectric-based solar still integrated with an evacuated tube collector utilizing an antibacterial-magnetic hybrid nanofluid. Desalination. 2021;500: 114871.
34. Visconti P, Primiceri P, Costantini P, Colangelo G, Cavalera G. Measurement and control system for thermosolar plant and performance comparison between traditional and nanofluid solar thermal collectors. Int J Smart Sens Intell Syst. 2016;9:1220–42.
35. Gianpiero C, Marco M, Arturo DR. Numerical simulation of thermal efficiency of an innovative Al_2O_3 nanofluid solar thermal collector: influence of nanoparticles concentration. Therm Sci. 2016;21:2769–79.
36. Colangelo G, Favale E, Miglietta P, Milanese M, de Risi A. Thermal conductivity, viscosity and stability of Al_2O_3-diathermic oil nanofluids for solar energy systems. Energy. 2016;95:124–36.
37. Narendran G, Gnanasekaran N, Perumal DA, et al. Integrated microchannel cooling for densely packed electronic components using vanadium pentaoxide (V2O5)-xerogel nanoplatelets-based nanofluids. J Therm Anal Calorim. 2023;148:2547–65.
38. Karki P, Perumal DA, Yadav AK. Comparative studies on air, water and nanofluids based Rayleigh-Benard natural convection using lattice Boltzmann method: CFD and exergy analysis. J Therm Anal Calorim. 2022;147:1487–503.
39. Xiong Q, Altnji S, Tayebi T, Izadi M, Hajjar A. A comprehensive review on the application of hybrid nanofluids in solar energy collectors. Sustain Energy Technol Assessments. 2021;47:101341.
40. Rashidi S, Karimi N, Mahian O. A concise review on the role of nanoparticles upon the productivity of solar desalination systems. Sustainable Energy Technol Assess. 2021;47: 101341.
41. Yang L, Ji W, Mao M, Huang J-N. An updated review on the properties, fabrication and application of hybrid-nanofluids along with their environmental effects. J Clean Prod. 2020;257: 120408.
42. Al-Kayiem HH, Mohamed MM. State of the Art of Hybrid Solar Stills for Desalination. Arabian J Sci Eng. 2023;48:5709–55.
43. Jathar LD, Ganesan S. Assessing the performance of concave type stepped solar still with nanoparticles and condensing cover cooling arrangement: an experimental approach. Groundwater Sustain Dev. 2021;12:100539.
44. Tuly SS, Sarker MRI, Das BK, Rahman MS. Effects of design and operational parameters on the performance of a solar distillation system: a comprehensive review. Groundwater Sustain Dev. 2021;14:100599.
45. Bait O. Enhanced heat and mass transfer in solar stills using nanofluids: a review. Sol Energy. 2018;170:694–722.
46. Iqbal A, Mahmoud MS, Sayed ET, Elsaid K, Abdelkareem MA, Hussain Alawadhi AG. Evaluation of the nanofluid-assisted desalination through solar stills in the last decade. J Environ Manag. 2021;277:111415.
47. Naveenkumar R, Gurumoorthy G, Kunjithapatham G. Impact of adding various nanomaterials in the efficiency of single slope solar still: a review. Mater Today: Proc. 2020;33:3942–6.
48. Akkala SR, Kaviti AK. Progress on suspended nanostructured engineering materials powered solar distillation- a review. Renew Sustain Energy Rev. 2021;143:110848.
49. Tiwari AK, Kumar V, Zafar Said HK, Paliwal,. A review on the application of hybrid nanofluids for parabolic trough collector: Recent progress and outlook. J Clean Product. 2021;292:126031.
50. Salman S, Abu Talib AR, Saadon S, Hameed Sultan MT. Hybrid nanofluid flow and heat transfer over backward and forward steps: a review. Powder Technol. 2020;363:448–72.
51. Guangtao Hu, Ning X, Hussain M, Sajjad U, Sultan M. Potential evaluation of hybrid nanofluids for solar thermal energy harvesting: a review of recent advances. Sustain Energy Technol Assess. 2021;48: 101651.
52. Syam Sundar L, Mesfin S, Sintie YT, Punnaiah V, Chamkha AJ, Sousa ACM. A review on the use of hybrid nanofluid in a solar flat plate and parabolic trough collectors and itsenhanced collector thermal efficiency. J Nanofluids. 2021;10:147–71.
53. Sharafeldin Mahmoud, Effects of Nanofluids on the Performance of Solar Collectors. Budapest University of Technology and Economics (Hungary), ProQuest Dissertations Publishing, 2020. 28680029
54. Mahbubul IM, Saidur R, Amalina MA, Elcioglu EB, Okutucu-Ozyurt T. Effective ultrasonication process for better colloidal dispersion of nanofluid. Ultrason Sonochem. 2015;26:361–9.